Proceedings of the Canadian Society for Mechanical Engineering International Congress
32nd Annual Conference of the Computational Fluid Dynamics Society of Canada
Canadian Society of Rheology Symposium
CSME/CFDSC/CSR 2025
May 25–28, 2025, Montréal, Québec, Canada

NUMBER

A simplified oscillating-foil turbine concept with an elliptical foil in pure heave

Alton Neid[1*], Pierre Fristot[2], Guy Dumas[1],

[1]CFD laboratory LMFN, Mechanical Engineering Department, Université Laval, Quebec, Canada
[2]OmegaWatt, Aurel, France
[*]Undergraduate research assistant, alton.neid.1@ulaval.ca

JANUARY 2025

***Abstract*—**This study explores a simplified oscillating-foil turbine concept with an elliptical foil in pure heave using two-dimensional (2D) simulations mostly at a chord-based Reynolds number of 3.0 x 10^6. Contrary to most concepts, the foil is oriented perpendicular to the upstream flow and is not pitching, simplifying the turbine's design. Three normalized heaving amplitudes are tested: 1.5, 5, and 15. Promising efficiencies up to over 45% (75% of the Betz limit of 59.3%) are found. Recommendations are made to potentially improve efficiency and power output in a future study.

***Keywords-component*—constrained oscillating-foil turbines; elliptical foil; large heaving amplitude; computational fluid dynamics**

I. INTRODUCTION

Free-stream turbines are clean energy producers that remain relatively underutilized. The oscillating-foil turbine (OFT) has performance potential in the same league as more traditional axial-flow turbines as well as the geometrical advantages of a rectangular power-extraction plane apt for riverbeds (although the concept can also be used for wind turbines) and simpler blades that are easier to manufacture. Many OFT concepts have been studied since the early 1980s [1] and even more intensely since the mid-2000s [2].

Classical OFT foils oscillate in heave (translation) and in pitch (rotation) as shown in Fig. 1 [3]. The present OFT study is pioneering because it considers a simplified and constrained (the motion is constrained at a given frequency and amplitude in heave, but the energy is entirely provided by the flow) OFT design with multiple potential advantages. Firstly, the pitching motion is eliminated, so the motion is pure heave. This removes the need for coupling of motions and simplifies the mechanical design of the turbine while improving its power transmission efficiency. Secondly, the foil is elliptical shaped, which makes it easier and cheaper to manufacture than NACA foils. OFTs with elliptical foils have been studied in the past [4, 5]. Thirdly, because it is constrained, the operating parameters can be completely controlled to optimize energy extraction in various flow conditions.

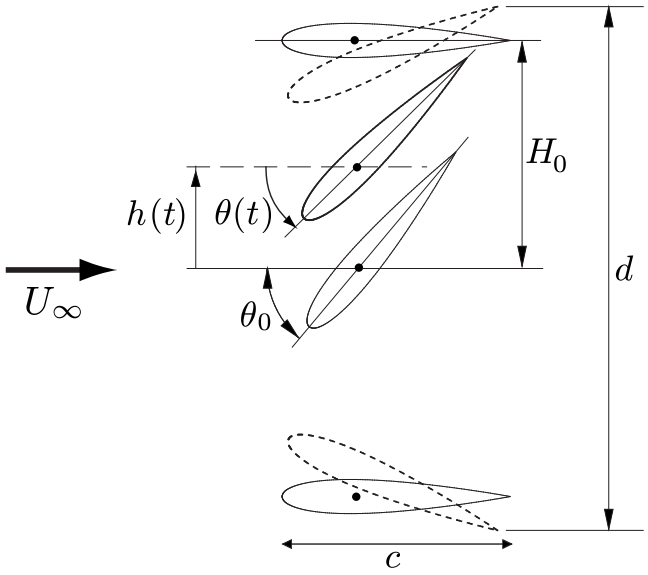


Figure. 1. Classical OFT concept with oscillations in heave and in pitch. Used with permission from [3].

This study also considers large heaving amplitudes up to 15 chord lengths. A previous study on a standard heave and

pitch OFT that looked at large heaving amplitudes (normalized heaving amplitudes up to 15) obtained 2D efficiencies as high as 0.49 [6]. With the removal of the pitching motion, we expect a reduction in efficiency and power output, although the reduction in manufacturing costs may outweigh those losses.

The objective of the present study is to explore the performance of an OFT concept with an elliptical foil in pure heave via 2D STAR-CCM+ simulations to see first of all if it can extract energy from the flow and second of all if its efficiency and power output can compete with more complex OFTs. Although this 2D study does not take into account three-dimensional (3D) effects, comparisons can be made to other OFT 2D studies and several previous studies [7, 8] have shown that the 3D performance of OFTs with endplates and an aspect ratio of 10 is about 90% of the 2D-predicted performance.

II. METHODOLOGY

A. Foil Geometry and Kinematics

The elliptical OFT concept explored in this 2D study uses an elliptical foil perpendicular to the flow as shown in Fig. 2. The heaving motion is constrained (controlled) and follows a sinusoidal function expressed by (1) where h is the heaving position, H_0 is the heaving amplitude, f is the heaving cycle frequency, and t is time. There is no pitching motion. Two elliptical foils are tested and shown in Fig. 3 and in Fig. 4. These two elliptical foils are referred to here as PF2412 and PF1206. The digits "2412" indicate the respective lengths of the semi-minor axes of 0.24 c and 0.12 c, while the digits "1206" indicate the respective lengths of the semi-minor axes of 0.12 c and 0.06 c. The thin side of the foil is upstream and the thick side is downstream.

$$h(t) = H_0 \sin(2\pi f t) \tag{1}$$

The simulations for the PF2412 foil are executed with normalized heaving amplitudes of $H_0/c = 1.5$, $H_0/c = 5$ and $H_0/c = 15$. $H_0/c = 5$ is tested for the PF1206 foil to compare two foils.

The choice of normalized frequency $f^* = fc/U_\infty$ of 0.16 for $H_0/c = 1.5$ is taken from the 2014 OFT study by Kinsey and Dumas [2]. The normalized frequencies for $H_0/c = 5$ ($f^* = 0.105$) and $H_0/c = 15$ ($f^* = 0.07$) are taken from the large heaving amplitude OFT study by Picard-Deland et al. [6]. Table I includes the normalized frequencies used in that study. No optimization of the normalized frequency is performed in the present study and remains something to be explored in the future.

B. Energy Extraction

For this OFT turbine concept in pure heave, the average power per cycle $\bar{P}$ is the time-average of the instantaneous power exchanged from the flow to the foil as expressed by (2). That instantaneous power is equal to the product of the force exerted on the foil by the fluid in the heaving (y) direction

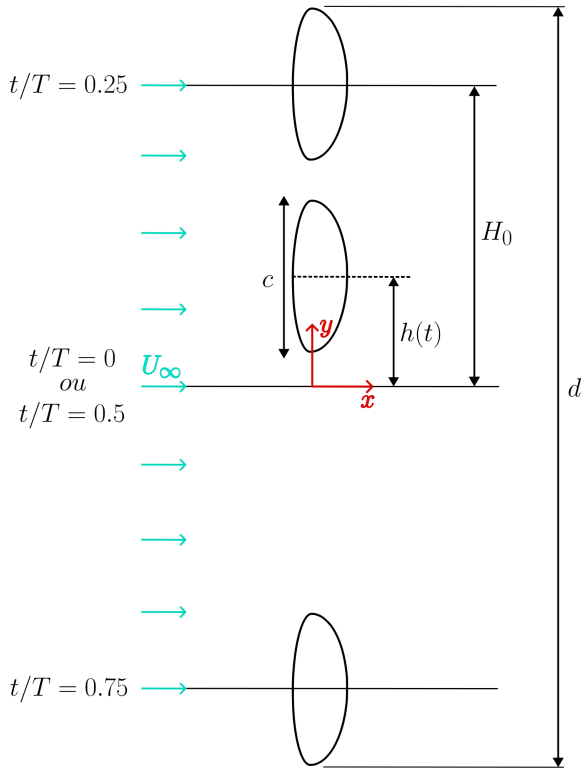


Figure. 2. Simplified oscillating-foil turbine concept with an elliptical foil in pure heave.

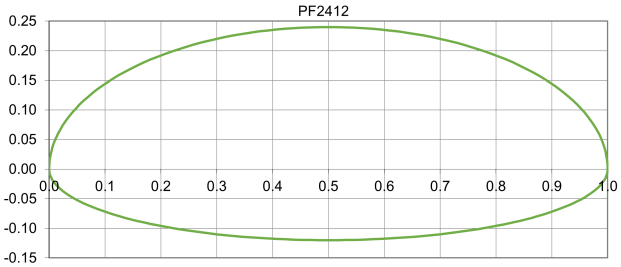


Figure. 3. PF2412 elliptical foil.

F_y and the heaving velocity V_y. T is the period of a heaving cycle (also equal to $1/f$) and t_i is the initial time of the cycle.

$$\bar{P} = \frac{1}{T}\int_{t_i}^{t_i+T} F_y V_y \, dt \tag{2}$$

Fig. 5 illustrates the effective fluid velocity V_{eff}, the effective angle of attack α, the lift force L, and the drag force D acting on the elliptical foil undergoing pure heave. At certain moments of the heaving cycle, the component of the lift force in the direction of the heaving velocity of the foil exceeds the component of the drag force acting in the

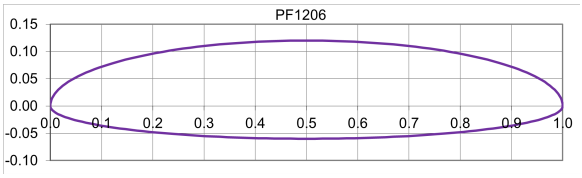


Figure. 4. PF1206 elliptical foil.

TABLE. I
NUMBER OF TIME STEPS PER CYCLE AND NORMALIZED FREQUENCIES AS A FUNCTION OF H_0/c FROM [6].

H_0/c	TS/cycle	f^*
1	2 000	0.14
3	2 000	0.12
5	3 000	0.105
10	5 000	0.08
15	8 000	0.07

direction opposite the heaving velocity of the foil. When this occurs, the foil is pulled in the direction of its velocity and instantaneous power is produced.

The average power coefficient per cycle $\overline{C_P}$ is defined in (3) where U_∞ is the upstream fluid velocity and b is the span of the foil (set at 1 meter to give a $\overline{C_P}$ per unit span in the present 2D simulations).

$$\overline{C_P} = \frac{\bar{P}}{\frac{1}{2}\rho U_\infty^3 bc} \tag{3}$$

The efficiency η is defined in (4) where d is the overall extent of the foil motion and equals $2H_0 + c$ for this OFT concept, as can be seen in Fig. 2.

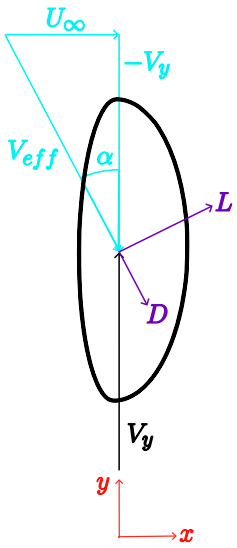


Figure. 5. Effective fluid velocity, effective angle of attack, lift force, and drag force acting on the elliptical foil in pure heave.

$$\eta = \frac{\bar{P}}{\frac{1}{2}\rho U_\infty^3 bd} \tag{4}$$

C. Numerics

The Unsteady Reynolds-averaged Navier–Stokes (URANS) 2D simulations in this study are carried out with STAR-CCM+ Version 2022.1.1 Build 17.02.008 [9], using an incompressible segregated flow solver and the *Implicit Unsteady* model. The one-equation *Spalart-Allmaras* turbulence model (with the *All y+ Wall Treatment* option) from the *Reynolds-Averaged-Navier-Stokes* model family is chosen for its good performance for flow around an oscillating airfoil [3].

The simulations use a chord c of 1 meter, a fluid density ρ of 1 kilogram per cubic meter, and an upstream velocity U_∞ of 1 meter per second to simplify the normalized variables. The kinematic viscosity ν is adjusted to give a chord-based Reynolds number ($Re = U_\infty c/\nu$) of 3.0×10^6 for all but one of the simulations because that Reynolds numbers is representative of a potential oscillating foil wind turbine application, and also because it ensures that all boundary layers may be considered fully turbulent. One simulation with the PF1206 foil is done at $Re = 5.0 \times 10^5$ to better compare with results from [6].

The computational domain, boundaries and meshes are shown in Fig. 6. The dimensions of the domain depend on the value of the heaving amplitude H_0/c to account for the large variation in the size of the swept area between cases at $H_0/c = 1.5$ and $H_0/c = 15$. This enables the confinement of the turbine with respect to the boundary conditions to be comparable between cases. The distances D_x and D_y are equal to $50\ H_0/c$ for all three cases of heave amplitude. The left boundary is a *Velocity Inlet* boundary condition of $1\ m/s$ from left to right and with a *Turbulent Viscosity Ratio* of 0.001 for the *Spalart-Allmaras* standard turbulence model. The flow domain is initialized with a uniform field corresponding to the inlet conditions. The top and bottom boundaries have *Symmetry Plane* boundary conditions. The right boundary has a *Pressure Outlet* boundary condition at $0\ Pa$ relative to the reference pressure. The surface of the elliptical foil is a no-slip wall boundary condition. The overset mesh function of STAR-CCM+ is used to superimpose the moving foil's mesh with the static background mesh. The background mesh is gradually made finer as it approaches the centre. The moving mesh is an approximately 49 000-cell structured mesh generated with ANSYS ICEM CFD Version 2023 R2 and has a first cell height of about 1.0×10^{-5}. The resulting y^+ has been verified to be of order $\mathcal{O}(1)$ over most of the cycles for all simulations.

The choice of simulation time steps is made according to the 2019 paper by Picard-Deland et al. [6] on the large heaving amplitude OFT. Picard-Deland et al. varied the time steps per cycle for various heaving amplitudes to preserve similar and low Courant numbers. The paper proposes values of the number of time steps per cycle $TS/cycle$ as a function of the value of H_0/c as presented in Table I.

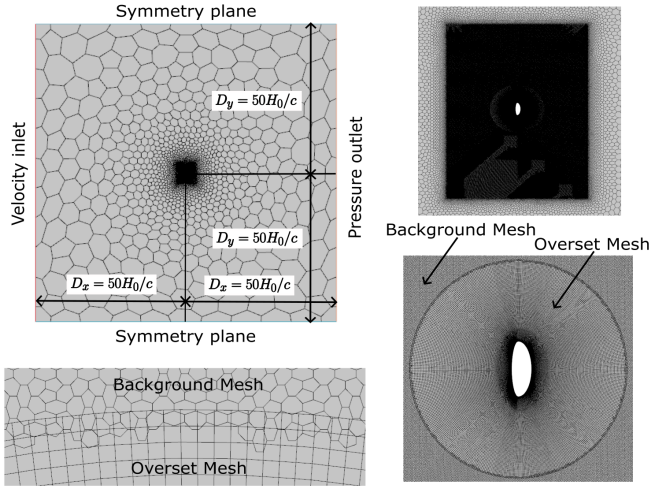


Figure. 6. Computational domain, boundaries and meshes.

TABLE. II
AVERAGE POWER COEFFICIENT ($\overline{C_P}$) AND EFFICIENCY (η) FOR VARIOUS CONSTRAINED OFT 2D SIMULATIONS. COMPARISON OF THIS STUDY WITH RESULTS OF SOME OF THE BEST CASES OF [6].

Foil	Pitching	Re	H_0/c	f^*	$\overline{C_P}$	η
PF2412	no	3.0×10^6	1.5	0.16	1.320[a]	0.330[a]
			5	0.105	3.503[b]	0.318[b]
			15	0.07	6.538[c]	0.211[c]
PF1206	no	3.0×10^6	5	0.105	4.956[d]	0.451[d]
		5.0×10^5	5	0.105	4.522[d]	0.411[d]
NACA 0020 (from [6])	yes	5.0×10^5	5	0.105	4.810[e]	0.449[e]
			15	0.07	13.489[e]	0.439[e]

[a]Average from cycles 3 to 11 (current study).

[b]Average from cycles 3 to 10 (current study).

[c]Average from cycles 3 to 7 (current study).

[d]Average over cycles 3 to 5 (current study).

[e]Theoretical asymptotic values from a best-fit curve from [6].

The simulation terminates its iterations at each time step if all the stopping criteria are met or if the maximum number of iterations (200 for this study) per time step is met. The stopping criteria and the normalized residuals (continuity, momentum in *x* and momentum in *y*) are set to a minimum of 10^{-5}. Also, asymptotic stopping criteria are set on the coefficient of force in the *x* direction and the coefficient of force in the *y* direction. For the two asymptotic stopping criteria, when the maximum difference in the last ten iterations is less than 0.001, the coefficient is considered converged.

D. Cycle-to-Cycle Convergence

The evolution of the average power coefficient $\overline{C_P}$ and the efficiency η per cycle can be monitored. The simulations in the present study have type 2 convergence patterns as identified by Kinsey and Dumas [2]. A type 2 convergence is defined as oscillations of the coefficient around an identifiable average due to complex vortex shedding that affects the foil differently from one cycle to another. Therefore, the $\overline{C_P}$ and η values in the results of this study are averages from the third cycle to the last cycle to consider the average while eliminating the turbine start-up.

E. Validation

To validate the numerical method presented above, a test case from the 2014 study on optimal operating parameters for an OFT by Kinsey and Dumas [2] was successfully reproduced within an acceptable margin of less than 4%. The test case is a sinusoidally constrained NACA 0015 foil with a pitching axis located at $1/3$ c from the leading edge, operating at $H_0/c = 1.5$, $f^* = 0.16$, a pitching amplitude $\theta_0 = 85$, a phase $\phi = 90$, and $Re = 500\ 000$. For the test case, the same numerical models, the same numerical strategy, and a very similar meshing strategy as the current study were used.

III. RESULTS AND DISCUSSION

Table II includes the average power coefficients $\overline{C_P}$ and efficiencies η for all of this study's simulations. For the present results, average values calculated from all completed cycles except the first two cycles are presented. Table II also includes a comparison with some best-case results from the large heaving amplitude OFT study by Picard-Deland et al. [6] which considered a NACA 0020 airfoil with imposed heave and pitch at a Reynolds number of 5.0×10^5.

Many observations can be made from Table II. This turbine concept with the PF2412 elliptical foil does indeed extract energy, but its performance is significantly lower than the optimal cases for other, more classical, OFTs such as the cases presented in [6].

As H_0/c increases, the average power coefficient is seen to increase while the efficiency decreases. However, more results with other values of H_0/c are needed to validate the extent of this trend. This trend is more present in the current study than in [6] where the pitch function was adjusted and optimized for each heave amplitude.

The PF2412 elliptical foil generates a lot of drag due to its large thickness and lack of tail. By comparing the simulations at $Re = 3.0 \times 10^6$ and $H_0/c = 5$, it can be observed that the thinner PF1206 foil gives significantly better performance than the PF2412 foil for that case. At $Re = 5.0 \times 10^5$, the PF1206 in pure heave without optimization reaches over 91% of the efficiency found in an optimized heaving and pitching OFT with a NACA 0020 foil from [6]. This is a very encouraging result for the potential application of this simplified OFT because the economical and manufacturing gains may outweigh the performance losses, especially when we consider that optimization was not carried out in the present study and that many parameters could indeed be optimized. To determine if the economical and manufacturing advantages of this OFT concept with an elliptical foil in pure heave could outweigh the decreased in performance, optimization and an

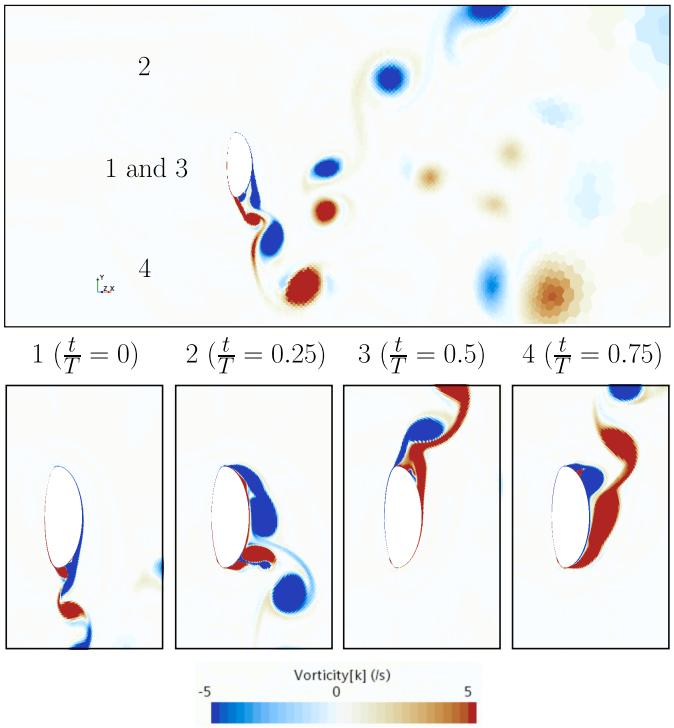


Figure. 7. Vorticity fields for the simplified OFT turbine concept with the PF2412 elliptical foil in pure heave with $H_0/c = 1.5$. Enlarged images for $t/T = 0$, $t/T = 0.25$, $t/T = 0.5$ and $t/T = 0.75$. Global image taken from the 20th cycle and enlarged images taken from the 22nd cycle.

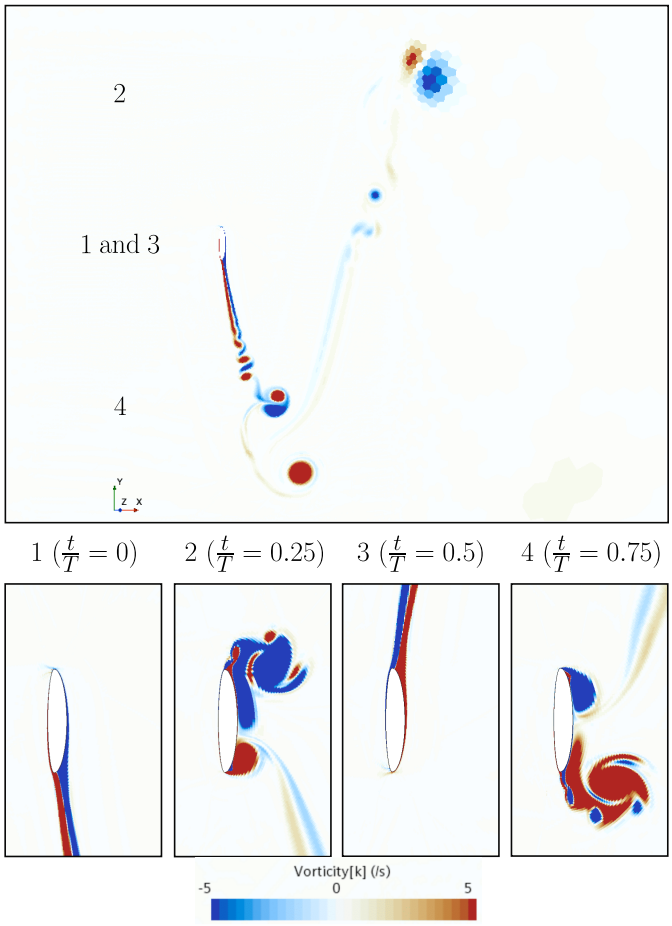


Figure. 8. Vorticity fields for the simplified OFT turbine concept with the PF1206 elliptical foil in pure heave with $H_0/c = 5$. Enlarged images for $t/T = 0$, $t/T = 0.25$, $t/T = 0.5$ and $t/T = 0.75$. Global image taken from the 7th cycle and enlarged images taken from the 7th cycle.

economical comparison with more traditional OFTs is needed.

Fig. 7 and Fig. 9 present vorticity fields for this OFT concept with the PF2412 elliptical foil in pure heave for $H_0/c = 1.5$ and $H_0/c = 15$ at certain cycles indicated in the titles of these figures. Enlarged images are included for $t/T = 0$, $t/T = 0.25$, $t/T = 0.5$ and $t/T = 0.75$. Fig. 8 presents the same for the PF1206 elliptical foil for $H_0/c = 5$. From the vorticity fields for the PF2412 elliptical foil, alternating swirling vortex shedding at the trailing edge of the foil can be observed, similar to a Kármán vortex street. Less alternating swirling vortex shedding is visible in the wake of the PF1206. In all three vorticity figures, an approximately sinusoidal wake is visible for about three-quarters of the cycle before dissipating. Larger flow separation is also observed for the PF2412 foil compared to the PF1206 foil. This partly explains the PF1206 foil's decreased drag in the heaving axis and improved efficiency (as is observed in Table II) compared to the PF2412 foil.

Among the numerous parameters of the present simplified turbine concept that could be optimized, let us mention the foil, the normalized frequency, the normalized heaving amplitude, and the heaving motion function. Several recommendations for potential improvements are given in the next paragraphs.

1) Foil: Since the energy extraction performance is better with the thinner PF1206 foil, it would be wise to test even thinner elliptical foils to find the optimal foil's thickness. Different aspect ratios of elliptical foils could also be explored in a future study.

2) Normalized Frequency: Different normalized frequencies are not tested in this study for the same H_0/c. This is an important aspect for future studies.

3) Normalized Heaving Amplitude: Because the average power coefficient per cycle $\overline{C_P}$ appears to increase with H_0/c, larger values of H_0/c should be explored if the goal is simply to maximize the $\overline{C_P}$ of a single turbine without regard to the efficiency η.

4) Heaving Motion Function: A large number of heaving motion functions could be explored beyond the sinusoidal one considered here. Some functions could result in different evolutions to the effective angle of attack that could potentially produce more power.

IV. CONCLUSION

Through two-dimensional simulations at a chord-based Reynolds number of 3.0 x 10^6 and at normalized heaving amplitudes of 1.5, 5, and 15, the present study showed that a simplified oscillating-foil turbine concept with an elliptical foil perpendicular to the flow in pure heave can not only

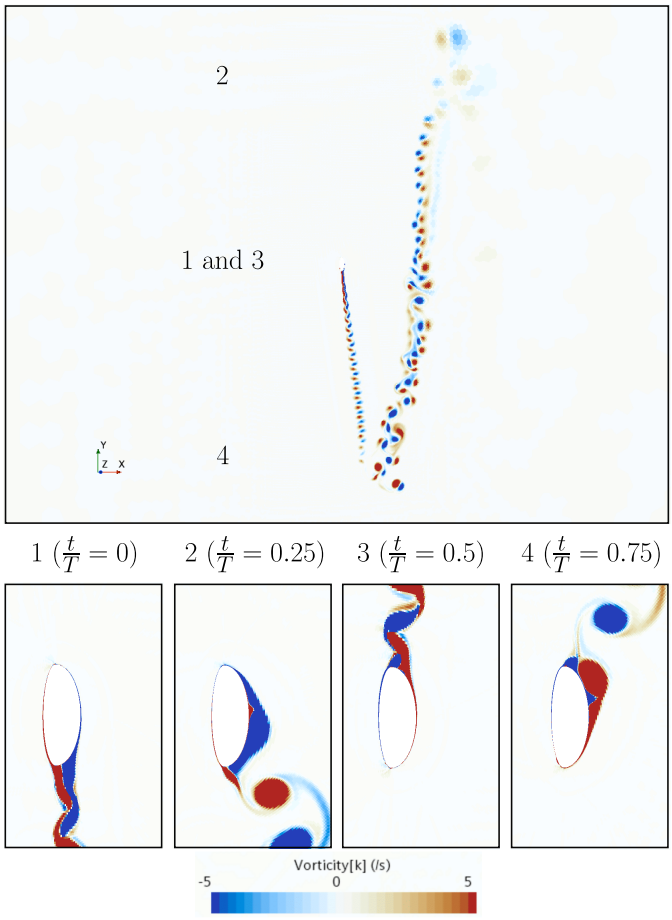


Figure. 9. Vorticity fields for the simplified OFT turbine concept with the PF2412 elliptical foil in pure heave with $H_0/c = 15$. Enlarged images for $t/T = 0$, $t/T = 0.25$, $t/T = 0.5$ and $t/T = 0.75$. Global image taken from the 7th cycle and enlarged images taken from the 8th cycle.

produce energy but do so at an efficiency greater than 45%. The power coefficient increases and the efficiency decreases in this study when the normalized heaving amplitude increases. The narrower PF1206 elliptical foil produced better results than the wider PF2412 elliptical foil for a normalized heaving amplitude of 5 (the only normalized heaving amplitude tested with the PF1206 foil). Although an efficiency of about 45% is slightly lower than the most efficient OFTs, no optimization of parameters was performed in this study; therefore, the concept could produce higher efficiencies and power coefficients after optimization. Furthermore, at a Reynolds number of 5.0 x 10^5, the studied OFT concept in pure heave with the PF1206 elliptical foil without optimization performs over 91% as well as an optimized heaving and pitching OFT with a NACA 0020 foil. It is important to note some of the advantages of a pure heave OFT that may outweigh the performance losses compared to a classical heave and pitch OFT: a simpler mechanical design, an improved power transmission efficiency, and easier and cheaper foil manufacturing. It is hoped that this preliminary study carried out in the context of an undergraduate summer internship will stimulate further optimization and economical investigations in the future for this promising new turbine concept.

ACKNOWLEDGEMENT

Thank you to Mr. Pierre Fristot of *OmegaWatt* in France for this idea, his encouragement, and funding for the 2019 large heaving amplitude study [6] at the LMFN which was used as inspiration for this study.

REFERENCES

[1] W. McKinney and J. DeLaurier, "The Wingmill: an oscillating-wing windmill," J. Energy, vol. 5, 1981, pp. 109–115.

[2] T. Kinsey and G. Dumas, "Optimal Operating Parameters for an Oscillating Foil Turbine at Reynolds Number 500,000," AIAA, vol. 52, no. 9, September 2014.

[3] T. Kinsey and G. Dumas, "Computational Fluid Dynamics Analysis of a Hydrokinetic Turbine Based on Oscillating Hydrofoils," Journal of Fluids Engineering, vol. 134, no 2, 2012.

[4] W. Jiang, D. Zhang, and Y.H. Xie, "Numerical investigation into the effects of arm motion and camber on a self-induced oscillating hydrofoil," Energy, vol. 115, 2016, pp. 1010-1021.

[5] J.S. Leontini, M.D. Griffith, D.L. Jacono, J. Sheridan, "Flow-Induced Vibration and Energy Harvesting Using Fully-Passive Flapping Foils," IUTAM Symposium on Recent Advances in Moving Boundary Problems in Mechanics, IUTAM Bookseries, vol. 34, Springer, March 2019.

[6] M. Picard-Deland, M. Olivier, G. Dumas, and T. Kinsey, "Oscillating-foil turbine operating at large heaving amplitudes", AIAA, vol. 57, no. 12, December 2019.

[7] T. Kinsey and G. Dumas, "Three-dimensional effects on an oscillating-foil hydrokinetic turbine," Journal of Fluids Engineering, vol. 134, no. 7, July 2012.

[8] J. Drofelnik and M.S. Campobasso, "Comparative turbulent three-dimensional Navier–Stokes hydrodynamic analysis and performance assessment of oscillating wings for renewable energy applications," International Journal of Marine Energy, vol. 16, 2016, 100–115.

[9] Siemens Digital Industries Software, "Simcenter STAR-CCM+ User Guide," Siemens, 2022.